Journal of Materials Chemistry B

RSC Publishing

PAPER

View Article Online
View Journal | View Issue

Combination of TNF-α and graphene oxide-loaded BEZ235 to enhance apoptosis of PIK3CA mutant colorectal cancer cells†

Cite this: *J. Mater. Chem. B*, 2013, **1**, 5602

Yuhua Cao,[abc] Yu Chong,[a] He Shen,[a] Mengxin Zhang,[a] Jie Huang,[a] Yimin Zhu[a] and Zhijun Zhang*[a]

The PI3K–AKT–mTOR pathway plays an important role in tumor cell growth, invasion, migration and apoptosis. A blockade of this signaling pathway has arisen as a compelling target for the tumor therapy. However, there is cross-talking between different signal pathways. Combined treatment of tumors with different signal pathway inhibitors is considered as an efficient strategy for cancer therapy. NVP-BEZ235 is a dual pan-class I PI3K and mTOR kinase inhibitor currently in clinical trial. TNF-α is involved in the regulation of cell apoptosis. In the current work, we explored the combined use of BEZ235 and TNF-α on the PIK3CA mutant colorectal cancer (CRC) cell proliferation inhibition. In our strategy, the BEZ235 is loaded on PEGylated graphene oxide (GO-PEG) by physisorption *via* π–π stacking to enhance its aqueous solubility. The resulting GO-BEZ235 complex exhibited excellent aqueous solubility while retaining a high cancer cell killing potency. The combination of BEZ235 and TNF-α shows an enhanced cellular proliferation inhibition for HCT 116 through enhancing the G1 phase arrest and cell apoptosis compared to either drug alone. Moreover, our experiments reveal that the enhanced tumor cell apoptosis depends on the activation of caspase-9, caspase-8 and caspase-3 mediated by the increased phosphorylation level of JNK. Taken together, our findings demonstrate for the first time the feasibility of BEZ235 delivered by GO-PEG and of the combined use of BEZ235 and TNF-α for PIK3CA mutant CRC therapy.

Received 30th May 2013
Accepted 19th August 2013

DOI: 10.1039/c3tb20764a

www.rsc.org/MaterialsB

Introduction

The phosphatidylinositol 3-kinases (PI3K), a family of lipid kinases, play important roles in regulating cell proliferation, motility, and survival. Class IA PI3K is composed of a p110α catalytic subunit and a p85 regulatory subunit activated by growth factor receptor tyrosine kinases (RTKs). The serine/threonine kinase AKT and mammalian target of rapamycin (mTOR) are the essential downstream mediators of the PI3K signaling pathway. AKT and mTOR collectively confer dominant survival signals *via* the respective downstream substrates that directly participate in cell apoptosis, cell cycle progression, and cellular translation.[1,2]

The PIK3CA gene, which encodes the catalytic subunit p110α, frequently mutates in many kinds of human cancers.[3] There are 20% of patients in colorectal cancer (CRC) carrying a PIK3CA mutation.[4] This mutation leads to growth factor independent p110α activation and confers constitutive kinase activity to promote tumor development and maintaining.[5,6] It has been reported that expression of the PIK3CA mutation gene in lung cells results in the development of lung cancer,[7] while tumor growth was delayed and decelerated in PIK3CA deficient mice. Further work showed that p110α regulated vessel integrity during tumorigenesis.[8] The PIK3CA mutation negatively regulated cell apoptosis as well. The PIK3CA mutation conferred resistance to growth factor deprivation stress (GFDS) induced apoptosis,[9] while inhibition of PI3K/AKT signaling sensitized cells to apoptotic stimuli, such as drug treatment or cellular stress.[10]

Because of the central role in the initiation and progression of tumors, the PI3K–mTOR signal pathway is a compelling target for tumor therapy.[11–14] However, a cell signal pathway is a complex network; inhibition of one pathway may induce compensatory signaling, which is a potential barrier to effective targeted cancer therapy.[15–18] To address this issue, a combination of inhibitors for the different pathways was employed for synergistic inhibition of cellular proliferation.[19–22] NVP-BEZ235 (BEZ235, Novartis), a dual pan-class I PI3K and mTOR kinase

[a]*Suzhou Key Laboratory of Nanobiomedicine, Division of Nanobiomedicine, Suzhou Institute of Nano-Tech and Nano-Bionics, Chinese Academy of Sciences, Suzhou 215123, China. E-mail: zjzhang2007@sinano.ac.cn; Fax: +86-0512-62603079; Tel: +86-0512-62872556*

[b]*University of Chinese Academy of Sciences, 19 Yuquan Road, Beijing, 100049, China*

[c]*Institute of Biophysics, Chinese Academy of Sciences, 15 Datun Road, Chaoyang District, Beijing, 100101, China*

† Electronic supplementary information (ESI) available. See DOI: 10.1039/c3tb20764a

inhibitor currently used in clinical trials, has been found to inhibit tumor growth in a number of different xenografts and genetically engineered mouse models.[22–25] Another study demonstrated that the tumor size in CRC xenograft mouse models decreased after treatment with BEZ235 alone, but there was not a corresponding cell apoptosis. This suggested that it is necessary to further investigate combination therapy of BEZ235 with other agents for CRC patients.[26] Mueller *et al.* showed that BEZ235 combined with irinotecan caused the synergistic induction of CRC cell apoptosis.[27]

TNF-α (tumor necrosis factor alpha) is the first cytokine used in cancer therapy. Binding to the TNF receptor type I (TNF-RI) promotes the recruitment of several intracellular adaptors,[28] while recruitment of death domain (DD) adaptors such as Fas associated DD (FADD) and TNF-R associated DD (TRADD) can lead to the activation of apoptosis signal pathways.[29] TNF-α at a low dose acts as a potent adjuvant for active antitumor immunotherapy.[30] The local administration of high-doses of TNF-α promotes anti-angiogenesis and has a powerful anti-tumor effect.[31] In the mice tumor model, increasing the TNF-α level leads to a reduction of tumor volume and weight.[32] However, the clinical use of TNF-α is hindered by its severe dose-dependent toxicity. To avoid such toxicity, regional administration is often used. An alternative strategy for the treatment for cancers with TNF-α is demanded. The combination of TNF-α with another drug may provide a good drug candidate for cancer therapy. A recent work by Park *et al.* indicated that the combination of IL-32 and TNF-α enhanced cell death in colorectal cancer.[32] Guan and colleagues found that the combination of TNF-α with IFN-γ enhanced the cell cycle arrest and apoptosis of OVCAR-3 and MCF-7 cells.[33] Moreover, the combination of 5-aminoimidazole-4-carboxamide riboside (AICAR) and TNF-α induced apoptosis of HCT116 cells.[34]

It is known that many potent, often aromatic, drugs are water insoluble, which has hampered their use for disease treatment. BEZ235 is a water insoluble aromatic drug; therefore, its practical application is limited to a large extent. To address this issue, many kinds of nanomaterials, such as micelles, liposomes, and inorganic nanoparticles have been used as vectors to enhance the drug solubility and drug delivery efficiency. Most recently, graphene oxide (GO) has attracted ever increasing interesting for drug delivery and other biomedical applications due to its good biocompatibility, ultrahigh drug loading capability, and the ease of surface functionalization.[35–37]

In this study, we explored the feasibility of a combined treatment by BEZ235 loaded on PEGylated GO (GO-PEG) and TNF-α for the growth-inhibition of the PIK3CA mutant CRC cells, and the possible mechanism for this effect. In our strategy, we utilized GO functionalized with amine-terminated six-armed PEG as a drug carrier for BEZ235, a poorly water soluble drug, to improve its aqueous solubility. We examined the growth-inhibitory effect of the GO-BEZ235 and TNF-α alone and in combination on HCT 116 cells. We found that GO-PEG could deliver BEZ235 into the cells efficiently, and a significant inhibitory effect of GO-BEZ235 on cell growth was observed. The combination of BEZ235 and TNF-α enhanced the G1 phase arrested and apoptosis of HCT 116 cells compared with the treatment with each alone. Moreover, we explored the molecular mechanism for this effect. We observed that the potentiation of the tumor cell apoptosis caused by the combined treatment of GO-BEZ235 and TNF-α depended on the enhancement of the phosphorylation level of JNK and activation of caspase-9, caspase-8, and caspase-3, which resulted in the cleavage of poly-ADP-ribose polymerase (PARP). It is expected that the combination of the PI3K–AKT–mTOR pathway inhibitor BEZ235 and TNF-α will offer a novel therapeutic strategy for PIK3CA mutant CRC.

Experimental section

Materials

Native graphite flakes were purchased from Alfa Aesar. Amine-terminated six-armed PEG was purchased from SunBio, *N*-(3-dimethylaminopropyl)-*N*′-ethylcarbodiimide (EDC), rhodamine B (RhB), and fluorescein isothiocyanate (FITC) were purchased from Sigma. BEZ235 was purchased from Selleck Chemicals, USA. SP sepharose Fast Flow, Q sepharose Fast Flow and sephacryl s-200 were purchased from GE Healthcare. Other reagents were purchased from China National Medicine Corporation and used as received.

Instruments

GO and GO-PEG were characterized by a Veeco Dimension 3100 atomic force microscope (AFM) and Tecnai G2 F20 S-Twin transmission electron microscope (TEM). The size and size distribution of the samples were determined by laser light scattering technique (Malvern The Zetasizer Nano ZS90). The loading capacity of BEZ235 on GO-PEG was examined by SHIMADZU UV-2550 spectrometer. Fluorescence spectra were obtained on a Hitachi F-4600 fluorescence spectrometer. Fluorescence microscopy images were captured by a laser confocal microscope (Nikon A1R). Cell lines were maintained in a water-jacketed CO_2 incubator (Thermo 3111). Results of MTT assay were read out from a PerkinElmer 2030 multilabel reader. Data of cell cycle and apoptosis were analyzed on a Beckman Coulter FC 500 flow cytometer. Western blotting images were taken by a FUJIFILM LAS4000-mini luminescent image analyzer.

Purification of TNF-α

The human TNF-α gene was cloned into a pET21a plasmid and expressed in *E. coli* BL21 (DE3) according to the R&D Systems Inc. product information of Recombinant Human TNF-α. Then the cell precipitates were suspended in lysis buffer (20 mM PB pH 7.4, 100 mM NaCl) and lysed by sonication. Following centrifugation at 12 000*g* for 30 min, the supernatant was dialyzed against SP sepharose Fast Flow binding buffer (50 mM PB pH 6.0, 50 mM NaCl). Then the supernatant was purified using SP sepharose Fast Flow and Q sepharose Fast Flow. The TNF-α purified by Q sepharose Fast Flow was then purified by sephacryl s-200. The purity of the TNF-α was measured by sodium dodecyl sulfate polyacrylamide gel electrophoresis (SDS-PAGE, 12%).

Synthesis of GO-PEG

GO was synthesized from expandable graphitic flakes (Graftech) using a modified Hummer's method,[38] and then modified with amine-terminated six-armed PEG molecules *via* EDC chemistry according to Liu *et al.*[39] The thus obtained GO-PEG was characterized by AFM, TEM and laser light scattering techniques. To monitor the cellular uptake, GO-PEG was labeled with RhB and FITC through physical adsorption to form GO-PEG-RhB and GO-PEG-FITC, respectively.

Loading of anticancer drug BEZ235

9 mL of 0.05 mg mL^{-1} GO-PEG in water was mixed with 1 mL of 0.5 mM DMSO solution of BEZ235 and stirred overnight at room temperature. Excessive BEZ235 was removed by centrifugation. The solution was centrifuged through a 100 kDa molecular weight cut-off filter (Millpore) and washed 5 times with water to remove free BEZ235 and DMSO. The retained solution in the filter was centrifuged at 23 447 *g* to remove the precipitate. The supernatant was GO-PEG-BEZ235 (GO-BEZ235) and stored at −20 °C for use. The loading of BEZ235 on GO-PEG was confirmed by UV-vis and fluorescence spectrometry. The concentration of BEZ235 was obtained by its absorption at 266 nm in the UV-vis spectrum (after subtracting the absorption contribution from GO-PEG).

Cell culture

Colorectal cancer cell lines HT-29 and HCT 116 (PIK3CA mutant), which were gifts from Professor Saijun Fan, Soochow University, were cultured at 37 °C in a 5% CO_2 atmosphere incubator in modified McCoy's 5A medium (sigma) complemented with 10% fetal bovine serum (FBS, Hyclone) and 1% penicillin–streptomycin. The monkey kidney epithelial (MA104) cell line, a gift from Professor Yuanding Chen (Institute of Medical Biology, Chinese Academy of Medical Sciences and Peking Union Medical College, Kunming, China), was maintained in Dulbecco's modified Eagle's medium with 10% FBS.

Cellular uptake of GO-PEG

HT-29, HCT 116 and MA104 cells were seeded into 6-well plates at densities of 2×10^5 cells per well and maintained for 24 h, then were incubated with GO-PEG-RhB for 2 h. After that, the cells were washed twice with PBS to remove the residual materials. A confocal fluorescence microscope was employed to test the cellular uptake of GO-PEG.

To investigate the cellular uptake pathway of GO-PEG, HCT 116 cells were incubated with GO-PEG for 18 h. To differentiate from the red fluorescence of the Lyso-Tracker, GO-PEG was labeled with FITC, which gives green emission. The cells were fixed by 4% paraformaldehyde and the lysosomes were label with Lyso-Tracker Red. Then, the cells were imaged by confocal fluorescence microscope.

Assessment of cell viability

HCT 116 cells were seeded into 96-well plates at densities of 3000 cells per well and maintained for 24 h. Next, the cells were incubated with GO-PEG, GO-BEZ235, and/or TNF-α with various concentrations for another 72 h in modified McCoy's 5A medium containing 10% FCS. Relative cell viability was measured by standard MTT assay.

Cell cycle arrest and apoptosis assay

HCT 116 cells were seeded into 6-well plates at densities of 1×10^5 cells per well and incubated with 40 nM GO-BEZ235, 40 nM BEZ235 and 80 ng mL^{-1} TNF-α, alone or in combination, at 24 h post seeding. After being incubated with the drug for another 24 h, floating cells in the medium were collected by centrifugation, while adherent cells were collected by treating with trypsin-EDTA. For the cell cycle arrest assay, after washing with PBS, cells were re-suspended in 70% ethanol for 24 h, and then stained with propidium iodide (Aldrich). After that, cells were analyzed by flow cytometry using CXP analysis software. For apoptosis assay, cells were stained with FITC-annexin V and propidium iodide following the standard protocol and then analyzed by flow cytometer.

Protein extraction and Western blotting

For biochemical characterization, 3×10^5 cells per well were seeded into 6-well plates and incubated for 24 h. After that, the medium was discarded and replaced with 2 mL per well of fresh medium without fetal bovine serum and starved for another 24 h. For the p-AKT S473 and PARP (Cell Signaling Technology) test, cells were then treated with GO-BEZ235 or TNF-α alone, or both in combination, for 6 h. After that, the cells were treated with EGF for 15 min. BEZ235 alone or in combination with TNF-α was used as a positive control. For caspase-3, caspase-8, caspase-9, P53, NF-κB, and p-JNK (all from Cell Signaling Technology) analysis, cells were treated with GO-BEZ235 or TNF-α alone, or both in combination, for 18 h. At the end of the incubation, the cells were collected and lysed with lysis buffer (50 mM Tris-Cl pH 6.8, 2% SDS, 10% glycerol, 1% β-ME). For the Western blotting assay, the protein samples were separated by SDS-PAGE and electro-transferred onto polyvinylidene fluoride (PVDF) membranes (Millipore). Monoclonal antibodies to p-AKT S47, PARP, caspase-3, caspase-8, caspase-9, NF-κB, p-JNK, P53 and β-actin (Beyotime Institute of Biotechnology) were used as primary antibodies. Second antibodies were either HRP-labeled goat anti-mouse IgG (H + L) or HRP-labeled goat anti-rabbit IgG (H + L). After that, proteins were visualized using an immobilonTM Western chemiluminescent HRP substrate kit (Millpore Cat no. WBKLS0050), and imaged by luminescent image analyzer (FUJIFILM) with multi gauge ver3 software.

Statistical analysis

Data for cell viability, cell cycle arrest and apoptosis assay were presented as mean ± SD from at least three independent experiments, which were done in triplicate each time. Statistical analysis was performed with Student's *t*-test (one-tailed). $p < 0.05$ was considered to be significant.

Results and discussion

Preparation of TNF-α, functional GO-PEG and loading of BEZ235 by GO-PEG

The purity of TNF-α was checked to be 92% by SDS-PAGE (data was not shown). The prepared GO was characterized by AFM technique, which revealed that most of the GO sheets are single to few-layered with a topographic height of 1–2 nm (Fig. S1a†). The PEGylation of GO led to the decrease in the size (Fig. S1a†), much smaller than that of GO. This is confirmed by TEM measurement (Fig. S1b†). Dynamic light scattering analysis indicates that the hydrodynamic diameter of GO-PEG was quite small, being about 49 nm.

BEZ235, which is a PI3K and mTOR kinase inhibitor, exhibits low aqueous solubility. In order to improve its aqueous solubility and to expand the application of this chemical drug, we employed amine-terminated six-armed PEG modified GO to load BEZ235. UV-vis and fluorescence spectra were measured to monitor the loading behavior. A comparative analysis of the absorption spectra of free BEZ235 and GO-PEG, and mixing of the two under certain conditions suggested the successful formation of a GO-BEZ235 complex (Fig. 1a). The binding between BEZ235 and GO is physical adsorption in nature, mainly *via* π–π stacking and hydrophobic interactions, as reported previously.[39,40] Fluorescence spectra confirmed that the formation of GO-BEZ235, as evidenced by the quenching of the fluorescence of BEZ235 after mixing of GO and BEZ235, due to energy transfer between BEZ235 and GO.[39] The adding of ethanol to the mixture led to the release of BEZ235 from the GO surface, and therefore observation of fluorescence recovery (Fig. 1b). The concentration of BEZ235 was determined by the absorption at 266 nm after subtracting the absorption contribution from GO-PEG. The drug loading ratio (the weight ratio of drug loaded to GO-PEG) was determined to be about 20%. As a result, the formation of GO-BEZ235 complexes significantly improved the solubility of BEZ235 (~0.5 mg mL^{-1} in terms of BEZ235), compared with that of the free BEZ235 (0.015 mg mL^{-1}), which is important for the clinical application of BEZ235. Furthermore, the physisorption of BEZ235 to GO will facilitate the release of BEZ235 from GO inside cells.

Cellular uptake of GO-PEG

The cellular uptake of GO-PEG is very important for its application in drug delivery. To understand the cellular uptake behavior, GO-PEG was labeled by RhB and then incubated with HCT 116, HT-29 and MA104 cells, respectively. As shown in Fig. S2,† after being incubated for 2 h, a red fluorescence signal was observed in all tested cells, indicating that GO-PEG could be internalized by the cells effectively. To elucidate the pathway for the internalization of GO-PEG, GO-PEG was labeled by FITC and incubated with HCT 116, in which the lysosomes were labeled by markers with red fluorescence. Fig. S3† shows that, after being incubated with the cells for 18 h, GO-PEG-FITC was located in the lysosome, suggesting that the internalization of GO-PEG was through lysosomes. The lysosomal matrix is acidic and it is favorable for drug release according to our previous work.[40]

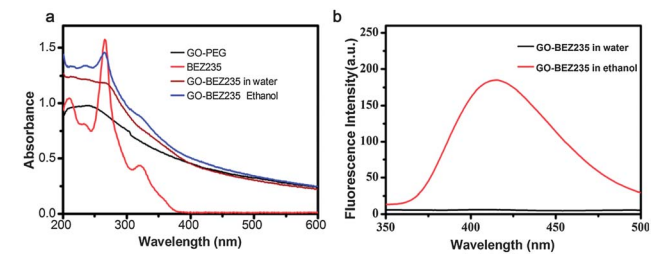

Fig. 1 Loading of BEZ235 on GO-PEG monitored by (a) UV-vis and (b) fluorescence spectra (excitation at 324 nm).

MTT assay

As a drug vector, the biocompatibility of GO-PEG is very important. MTT assay (Fig. 2a) indicated that GO-PEG has no toxicity to HCT 116 cells even with GO-PEG concentrations up to 100 μg mL^{-1}. To examine the inhibitory effect of the drug on cell growth, HCT 116 cells were incubated with GO-BEZ235 and TNF-α, either alone or in combination, at different concentrations. The results from the MTT assay (Fig. 2b) showed that, TNF-α had little cytotoxic effect on HCT 116 even at concentrations up to 160 ng mL^{-1} (about 20% cellular proliferation inhibition comparing to control), which was consistent with the previous report by other researchers.[41] The treatment by GO-BEZ235 suppressed HCT 116 cell growth effectively, with the IC50 23 ± 0.85 nM (Fig. 2c), indicating that BEZ235 loaded on GO still kept its highly potent cancer cell killing capacity (IC50 for free BEZ235 is about 20 nM, data was not shown). When combined with TNF-α, the IC50 value decreased significantly (15.5 ± 0.34 nM, Fig. 2c, $p < 0.05$). Clearly, the combined

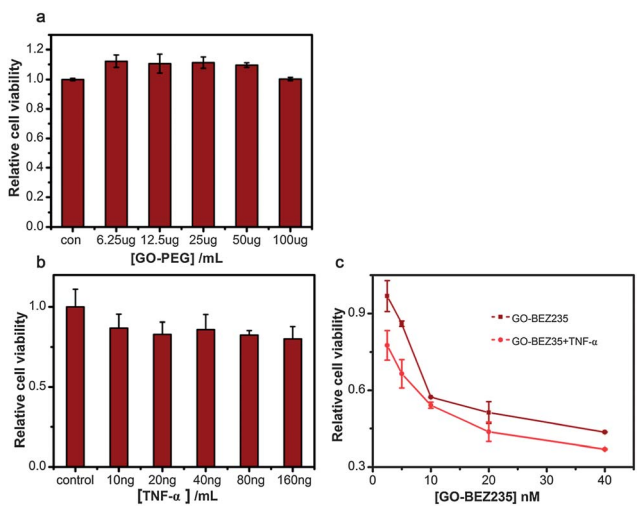

Fig. 2 The proliferation of HCT 116 cells was affected (a) by GO-PEG; (b) by TNF-α; (c) either by GO-BEZ235 alone or in combination with TNF-α (at the ration of 2 : 1, TNF-α ng mL^{-1}: GO-BEZ235 nM) at different concentrations monitored by MTT assay. The results are expressed as mean ± SD ($n = 3$). The IC50 of GO-BEZ235 to HCT 116 cells is about 23 ± 0.85 nM, the IC50 of GO-BEZ235 + TNF-α is about 15.5 ± 0.34 nM, $p < 0.05$.

treatment with GO-BEZ235 and TNF-α was more effective in cell growth inhibition than either drug alone.

Cell cycle arrest and apoptosis of HCT 116 cells

To unveil the mechanism of the enhanced proliferation suppression of colorectal cancer cells by the combination of the two drugs, HCT 116 cells were incubated with the drugs and then stained with propidium iodide for the cell cycle arrest assay. As shown in Fig. 3a and b, the combination of BEZ235 and TNF-α induced a significant accumulation of cells in the G1 phase and a concomitant decrease in the S phase compared to the treatment by either drug alone ($p < 0.05$). Meanwhile, the combination of the BEZ235 and TNF-α increased the number of sub-G1 events indicative of apoptotic cells. Low levels of G1 phase and sub-G1 events were detected for the treatment with GO-BEZ235, BEZ235 or TNF-α alone. An Annexin V–propidium iodide stain was further performed to examine the level of cell apoptosis. As shown in Fig. 3c and d, GO-BEZ235 or BEZ235 had a weak effect on the apoptosis of HCT 116 cells. This result was in good agreement with an earlier report by Roper J *et al.*[26] The percentages of apoptotic cells treated with DMSO (control), TNF-α, BEZ235, and GO-BEZ235 were determined to be (6.1 ± 0.6)%, (13.7 ± 0.55)%, (12.95 ± 0.66)%, and (10.55 ± 2.33)%, respectively. In contrast, the percentage of the cell apoptosis induced by the combined treatment of free BEZ235 and TNF-α was much higher, being up to (42 ± 9.05)%, clearly indicating a strong synergetic effect of BEZ235 and TNF-α on the cell apoptosis of HCT 116 cells. This result was consistent with the sub-G1

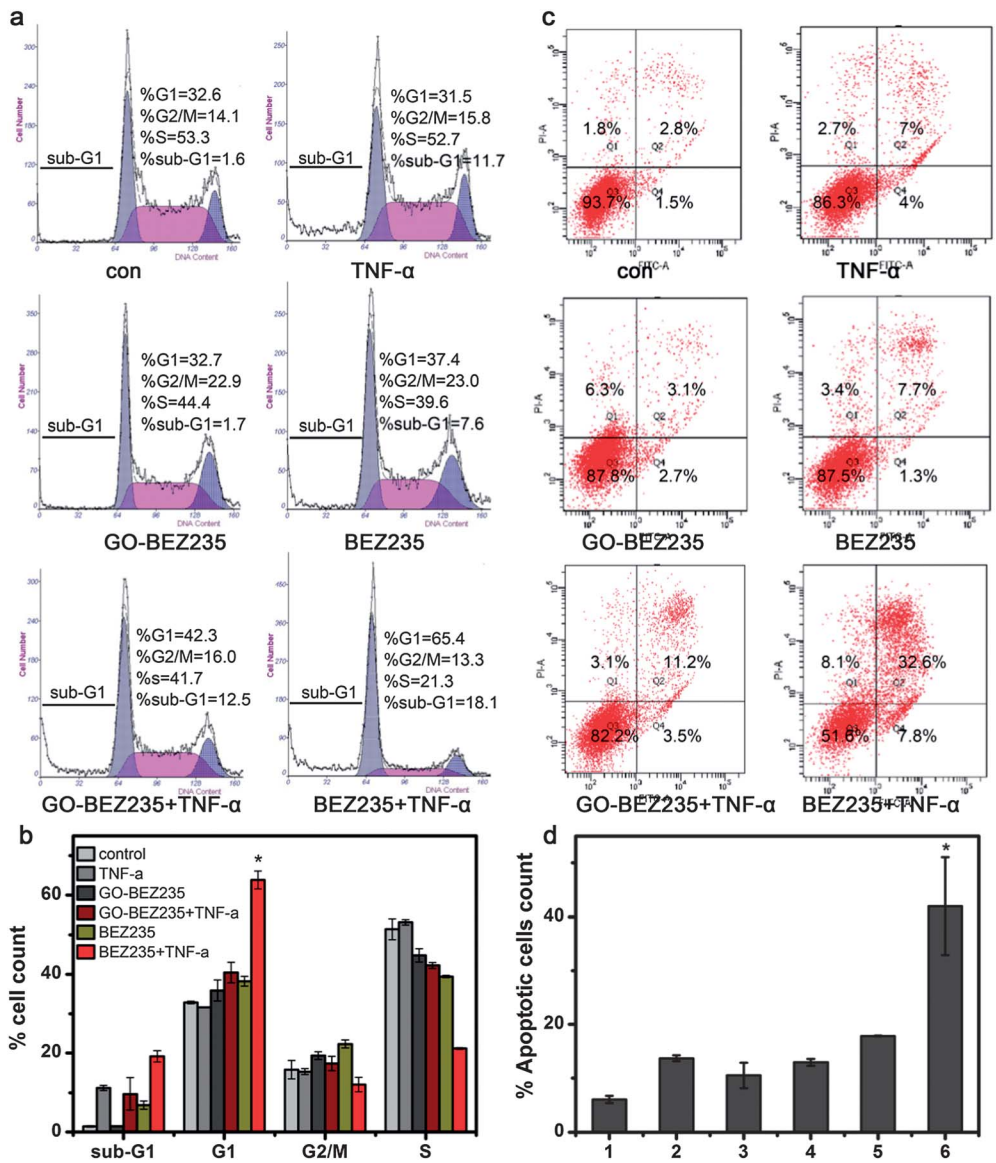

Fig. 3 Flow cytometric analysis of cell cycle arrest and apoptosis induced by BEZ235 and TNF-α alone or combination. (a) The cell cycle analysis of HCT 116 cells treated with DMSO, TNF-α, BEZ235, or the combination of BEZ235 and TNF-α by flow cytometry. (b) The percentage of cell phases. (c) The apoptosis of HCT 116 induced by the combination treatment of BEZ235 and TNF-α. (d) Plot of apoptosis levels. 1: control; 2: TNF-α; 3: GO-BEZ235; 4: BEZ235; 5: GO-BEZ235 + TNF-α; 6: BEZ235 + TNF-α. The results were expressed as mean ± SD ($n = 3$). *$p < 0.05$ *versus* cells treated with BEZ235 or TNF-α.

quantification in the cell cycle analysis. Lower level cell apoptosis (about 17.8% to total cells) and G1 phase arrest (about 42.3% to total cells) were detected in HCT 116 cells with the combined treatment of GO-BEZ235 and TNF-α compared with the combination of free BEZ235 and TNF-α, probably due to the fact that the release of BEZ235 from GO to the cytoplasm was slower than the free BEZ235, since free BEZ235 is liposoluble, therefore released into the cytoplasm faster than the GO-loaded BEZ235.

Phosphorylation level of AKT

To investigate the molecular mechanism for the cell cycle arrest and the enhanced apoptosis of HCT 116 cells induced by the combined treatment of GO-BEZ235 and TNF-α, Western blotting assay was performed to examine the changes in the AKT phosphorylation, a major downstream effector of the PI3K and mTOR. AKT regulates cell growth and survival pathways by phosphorylating substrates such as GSK3, fork-head transcription factors, and the TSC2 tumor suppressor protein.[42] As shown in Fig. 4a and b, for HCT 116 cells, treating with each drug alone or both in combination led to a decrease in the level of p-AKT S473. Co-treatment attenuated the inhibition of AKT S473 phosphorylation comparing to either drug alone. A previous report by Xia *et al.* showed that TNF-α could induce the proliferation, differentiation and survival of cells through activation of the AKT and ERK1/2.[43] Ehrenschwender and his colleagues also demonstrated that stimulation with Fc-CD95L and TNF-α further increased AKT phosphorylation in HCT 116 PIK3CA-mutant cells.[20] Therefore it is speculated that TNF-α may play a dominant role in the phosphorylation of AKT S473.

Phosphorylation of JNK and activation of caspases

Apoptosis is an important program for eliminating unwanted cells in a lot of physiological processes. Regulation of this process is implicated in the pathogenesis of many cancer developments. TNF-α is a pro-inflammatory cytokine, which exerts its biological functions by activating multiple downstream signaling pathways, including caspases, IκB kinase (IKK) and c-Jun N-terminal protein kinase (JNK). In this study, the underlying signal transduction pathway that resulting in cell apoptosis by TNF-α was evaluated. JNK is a member of the mitogen activated protein kinase (MAPK) superfamily. Some previous studies showed that JNK could phosphorylate transcription factors including P53 to regulate their activities and act as a pro-apoptotic kinase.[44,45] As shown in Fig. 5a and b, both GO-BEZ235 and TNF-α induced an increased phosphorylation level of the JNK compared to that of the negative control. TNF-α caused a dose-dependent increase in JNK phosphorylation level. The combination of the two drugs enhanced this effect, which was consistent with the result for the combination of free BEZ235 and TNF-α (Fig. 5a and b). JNK was activated through phosphorylation, resulting in the activation of caspase signals to initiate a protease cascade.

Caspase activation is usually a feature of cell apoptosis. Caspase-8 lies at the apex of an apoptotic cascade and initiates proteolytic activation of downstream caspase family members, such as caspase-3 and caspase-7, thereby triggering the execution steps of apoptosis. Previous work indicated that the combination of PI3K and an mTOR inhibitor increased the activation of caspase-8 and caspase-3.[46] Astragalus membranaceus (AST), which down-regulated mTOR, exhibited enhanced activation of caspase-8 by combination with TNF-α.[47] Herein, in this study, the activation of caspase-8, caspase-9, caspase-3 and cleaved caspase-3 substrate PARP was investigated using Western blotting analysis. As shown in Fig. 4a and c and 5a and c–f, GO-BEZ235 imposed a weak effect on the activation of caspase-8, caspase-9, caspase-3 and the cleavage of

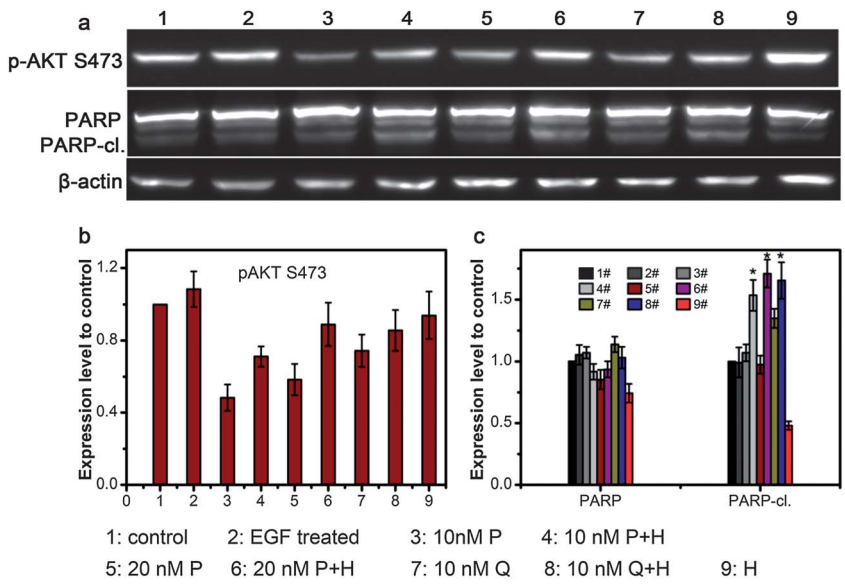

Fig. 4 The analysis of AKT S473 phosphorylation and PARP cleavage affected by various drugs. (a) Representative Western blotting results of the phosphorylation of AKT S473 and the cleavage of PARP when cells were treated with various drugs, (b) quantitative plot for the AKT phosphorylation and (c) quantitative plot for PARP cleavage. P: GO-BEZ235; Q: BEZ235; H: 80 ng mL^{-1} TNF-α. The results were expressed as mean ± SD ($n = 3$). *$p < 0.05$ *versus* cells treated with one drug alone.

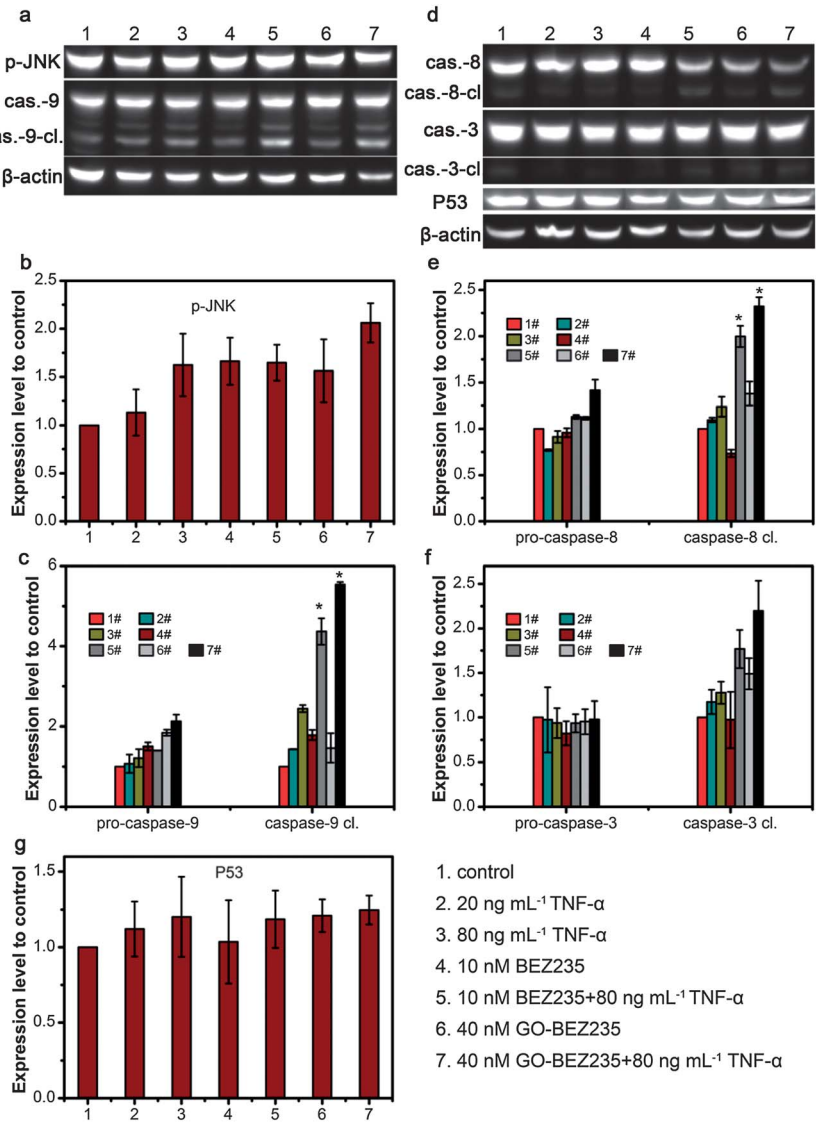

Fig. 5 The effect of various drugs on the PI3K and TNF-α apoptotic pathway of HCT 116. Western blotting assay of (a) the phosphorylation of JNK, and cleavage of caspase-9, (d) cleavages of caspase-8 and caspase-3, and expression of P53 when cells were treated with different drugs. Quantitative plots of (b) phosphorylation of JNK, cleavages of (c) caspase-9, (e) caspase-8, and (f) caspase-3, and (g) expression of P53. The results were expressed as mean ± SD ($n = 3$). *$p < 0.05$ *versus* cells treated with one drug alone.

PARP. This indicated that GO-BEZ235 had little effect on apoptosis, which was consistent with the observation for the free BEZ235 in this study and other reports.[26] TNF-α also showed a weak effect on caspase activation and PARP cleavage in this study, which was consistent with another report.[48] However, the combination of these two drugs significantly enhanced the proteolysis of caspase-8, caspase-9, and caspase-3. Previous study by Su *et al.* also indicated that 5-amino-imidazole-4-carboxamide riboside (AICAR) co-treatment with TNF-α enhanced activities of caspase-8, caspase-9, and caspase-3 resulting in HCT 116 cell apoptosis.[34] Another study indicated that the mTOR inhibitior AST enhanced the apoptotic cascade led by TNF-α through active caspase 8 and caspase 3.[47] Antofine enhanced the pro-apoptotic effect of TNF-α and also led to the cleavage PARP and caspase 8.[48] All these results suggested that the combination of GO-BEZ235 and TNF-α modulates the extrinsic apoptotic cascade leading the cellular proliferation inhibition.

The tumor suppressor protein P53 regulates the expression of genes to mediate cell cycle arrest and the apoptosis procedure in cells. As shown in Fig. 5d and g, GO-BEZ235, BEZ235 and TNF-α alone or in combination increased the level of total P53, indicating the involvement of P53 in cellular proliferation inhibition. Moreover, the Western blotting assay showed that the treatment by either drug alone or in combination had no effect on the NF-kB level (data was not shown).

Based on the discussion above, we proposed a model for the HCT 116 cell apoptosis induced by the combined treatment of the two drugs, which is shown in Fig. 6. Given the results above, it seems reasonable to postulate that the increases of JNK

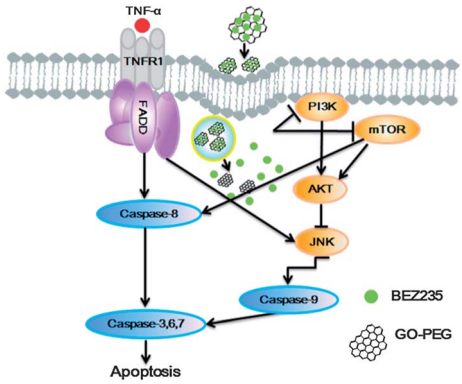

Fig. 6 Schematic showing the proposed apoptotic pathway in HCT 116 cells treated by a combination of GO-BEZ235 and TNF-α.

phosphorylation and caspase activation are the main reasons for the enhancement of HCT 116 cell proliferation inhibition.

Conclusion

In summary, we have developed GO-PEG as a delivery vector for BEZ235, and investigated the effect of the combined treatment with GO-BEZ235 and TNF-α on the HCT 116 cell growth. We have demonstrated that the combination of GO-BEZ235 and TNF-α significantly enhanced the HCT 116 programmed cell death, depending on the increase in the JNK phosphorylation level and activation of caspase-9, caspase-8 and caspase-3. Taken together, the current work demonstrated for the first time the possibility of BEZ235 delivered by GO-PEG and the combination of dual PI3K–mTOR inhibitor BEZ235 and TNF-α for PIK3CA mutant CRC therapy.

Acknowledgements

Financial support of this work by Natural Science Foundation of China (no. 51361130033, 21073224) and National Basic Research Program of China (no. 2010CB933504) are gratefully acknowledged.

References

1 J. E. Thompson and C. B. Thompson, *J. Clin. Oncol.*, 2004, **22**, 4217–4226.
2 D. C. Fingar and J. Blenis, *Oncogene*, 2004, **23**, 3151–3171.
3 Y. Samuels, Z. H. Wang, A. Bardelli, N. Silliman, J. Ptak, S. Szabo, H. Yan, A. Gazdar, S. M. Powell, G. J. Riggins, J. K. V. Willson, S. Markowitz, K. W. Kinzler, B. Vogelstein and V. E. Velculescu, *Science*, 2004, **304**, 554–554.
4 S. Velho, C. Oliveira, A. Ferreira, A. C. Ferreira, G. Suriano, S. Schwartz, Jr, A. Duval, F. Carneiro, J. C. Machado, R. Hamelin and R. Seruca, *Eur. J. Cancer*, 2005, **41**, 1649–1654.
5 C. H. Huang, D. Mandelker, O. Schmidt-Kittler, Y. Samuels, V. E. Velculescu, K. W. Kinzler, B. Vogelstein, S. B. Gabelli and L. M. Amzel, *Science*, 2007, **318**, 1744–1748.
6 N. Miled, Y. Yan, W. C. Hon, O. Perisic, M. Zvelebil, Y. Inbar, D. Schneidman-Duhovny, H. J. Wolfson, J. M. Backer and R. L. Williams, *Science*, 2007, **317**, 239–242.
7 J. A. Engelman, L. Chen, X. H. Tan, K. Crosby, A. R. Guimaraes, R. Upadhyay, M. Maira, K. McNamara, S. A. Perera, Y. C. Song, L. R. Chirieac, R. Kaur, A. Lightbown, J. Simendinger, T. Li, R. F. Padera, C. Garcia-Echeverria, R. Weissleder, U. Mahmood, L. C. Cantley and K. K. Wong, *Nat. Med.*, 2008, **14**, 1351–1356.
8 T. L. Yuan, H. S. Choi, A. Matsui, C. Benes, E. Lifshits, J. Luo, J. V. Frangioni and L. C. Cantley, *Proc. Natl. Acad. Sci. U. S. A.*, 2008, **105**, 9739–9744.
9 X. N. Guo, A. Rajput, R. Rose, J. Hauser, A. Beko, K. Kuropatwinski, C. Levea, R. M. Hoffman, N. G. Brattain and J. Wang, *Cancer Res.*, 2007, **67**, 5851–5858.
10 R. J. Yao and G. M. Cooper, *Science*, 1995, **267**, 2003–2006.
11 T. Fujishita, M. Aoki and M. M. Taketo, *Cell Cycle*, 2009, **8**, 3684–3687.
12 D. A. Guertin and D. M. Sabatini, *Cancer Cell*, 2007, **12**, 9–22.
13 P. X. Liu, H. L. Cheng, T. M. Roberts and J. J. Zhao, *Nat. Rev. Drug Discovery*, 2009, **8**, 627–644.
14 T. D. Bunney and M. Katan, *Nat. Rev. Cancer*, 2010, **10**, 342–352.
15 P. R. Somanath, J. Vijai, J. V. Kichina, T. Byzova and E. S. Kandel, *Oncogene*, 2009, **28**, 2365–2369.
16 Q. B. She, E. Halilovic, Q. Ye, W. Zhen, S. Shirasawa, T. Sasazuki, D. B. Solit and N. Rosen, *Cancer Cell*, 2010, **18**, 39–51.
17 M. Cheung, A. Sharma, S. V. Madhunapantula and G. P. Robertson, *Cancer Res.*, 2008, **68**, 3429–3439.
18 A. Carracedo, L. Ma, J. Teruya-Feldstein, F. Rojo, L. Salmena, A. Alimonti, A. Egia, A. T. Sasaki, G. Thomas and S. C. Kozma, *J. Clin. Invest.*, 2008, **118**, 3065–3074.
19 A. Prahallad, C. Sun, S. Huang, F. Di Nicolantonio, R. Salazar, D. Zecchin, R. L. Beijersbergen, A. Bardelli and R. Bernards, *Nature*, 2012, **483**, 100–103.
20 M. Ehrenschwender, D. Siegmund, A. Wicovsky, M. Kracht, O. Dittrich-Breiholz, V. Spindler, J. Waschke, H. Kalthoff, A. Trauzold and H. Wajant, *Cell Death Differ.*, 2010, **17**, 1435–1447.
21 K. Zitzmann, E. De Toni, J. von Rüden, S. Brand, B. Göke, R. P. Laubender and C. J. Auernhammer, *Endocr. Relat. Cancer*, 2011, **18**, 277–285.
22 D. Roulin, L. Waselle, A. Dormond-Meuwly, M. Dufour, N. Demartines and O. Dormond, *Mol. Cancer*, 2011, **10**, 90.
23 D. C. Cho, M. B. Cohen, D. J. Panka, M. Collins, M. Ghebremichael, M. B. Atkins, S. Signoretti and J. W. Mier, *Clin. Cancer Res.*, 2010, **16**, 3628–3638.
24 P. M. Bhende, S. I. Park, M. S. Lim, D. P. Dittmer and B. Damania, *Leukemia*, 2010, **24**, 1781–1784.
25 C. Brünner-Kubath, W. Shabbir, V. Saferding, R. Wagner, C. F. Singer, P. Valent, W. Berger, B. Marian, C. C. Zielinski, M. Grusch and T. W. Grunt, *Breast Cancer Res. Treat.*, 2011, **129**, 387–400.
26 J. Roper, M. P. Richardson, W. V. Wang, L. G. Richard, W. Chen, E. M. Coffee, M. J. Sinnamon, L. Lee, P. C. Chen, R. T. Bronson, E. S. Martin and K. E. Hung, *PLoS One*, 2011, **6**, e25132.

27 A. Mueller, E. Bachmann, M. Linnig, K. Khillimberger, C. C. Schimanski, P. R. Galle and M. Moehler, *Cancer Chemother. Pharmacol.*, 2012, **69**, 1601–1615.
28 P. W. Dempsey, S. E. Doyle, J. Q. He and G. Cheng, *Cytokine Growth Factor Rev.*, 2003, **14**, 193–209.
29 J. Han, R. C. Soletti, A. Sadarangani, P. Sridevi, M. E. Ramirez, L. Eckmann, H. L. Borges and J. Y. Wang, *Mol. Cancer Res.*, 2013, **11**, 207–218.
30 A. Johansson, J. Hamzah, C. J. Payne and R. Ganss, *Proc. Natl. Acad. Sci. U. S. A.*, 2012, **109**, 7841–7846.
31 F. J. Lejeune, C. Rüegg and D. Liénard, *Curr. Opin. Immunol.*, 1998, **10**, 573–580.
32 E. S. Park, J. M. Yoo, H. S. Yoo, D. Y. Yoon, Y. P. Yun and J. Hong, *Mol. Carcinog.*, 2012, DOI: 10.1002/mc.21990.
33 Y. Q. Guan, Z. Li, A. Yang, Z. Huang, Z. Zheng, L. Zhang, L. Li and J. M. Liu, *Biomaterials*, 2012, **33**, 6162–6171.
34 R. Y. Su, Y. Chao, T. Y. Chen, D. Y. Huang and W. W. Lin, *Mol. Cancer Ther.*, 2007, **6**, 1562–1571.
35 L. Feng, X. Yang, X. Shi, X. Tan, R. Peng, J. Wang and Z. Liu, *Small*, 2013, **9**, 1989–1997.
36 X. Shi, H. Gong, Y. Li, C. Wang, L. Cheng and Z. Liu, *Biomaterials*, 2013, **34**, 4786–4793.
37 K. Yang, L. Z. Feng, X. Z. Shi and Z. Liu, *Chem. Soc. Rev.*, 2013, **42**, 530–547.
38 W. S. Hummers Jr and R. E. Offeman, *J. Am. Chem. Soc.*, 1958, **80**, 1339–1339.
39 Z. Liu, J. T. Robinson, X. Sun and H. Dai, *J. Am. Chem. Soc.*, 2008, **130**, 10876–10877.
40 L. Zhang, J. Xia, Q. Zhao, L. Liu and Z. Zhang, *Small*, 2010, **6**, 537–544.
41 M. Farah, K. Parhar, M. Moussavi, S. Eivemark and B. Salh, *Am. J. Physiol.: Gastrointest. Liver Physiol.*, 2003, **285**, G919–G928.
42 I. Vivanco and C. L. Sawyers, *Nat. Rev. Cancer*, 2002, **2**, 489–501.
43 Z. Xia, M. Dickens, J. Raingeaud, R. J. Davis and M. E. Greenberg, *Science*, 1995, **270**, 1326–1331.
44 R. J. Davis, *Cell*, 2000, **103**, 239–252.
45 A. Lin, *BioEssays*, 2002, **25**, 17–24.
46 F. E. Bertrand, J. D. Spengemen, J. G. Shelton and J. A. McCubrey, *Leukemia*, 2004, **19**, 98–102.
47 K. K. W. Auyeung, N. L. Mok, C. M. Wong, C. H. Cho and J. K. S. Ko, *Int. J. Mol. Med.*, 2010, **26**, 341–349.
48 H. Y. Min, H. J. Chung, E. H. Kim, S. Kim, E. J. Park and S. K. Lee, *Biochem. Pharmacol.*, 2010, **80**, 1356–1364.